Review of cardiovascular imaging in the Journal of Nuclear Cardiology 2020: positron emission tomography, computed tomography, and magnetic resonance

Wael A. AlJaroudi, MD, FASNC,[a] and Fadi G. Hage, MD, MASNC[b,c]

[a] Division of Cardiovascular Medicine, Augusta University, Augusta, GA
[b] Division of Cardiovascular Disease, Department of Medicine, University of Alabama at Birmingham, Birmingham, AL
[c] Section of Cardiology, Birmingham Veterans Affairs Medical Center, Birmingham, AL

Received May 19, 2021; accepted May 19, 2021
doi:10.1007/s12350-021-02685-9

Although the year 2020 was different from other years in many respects, the *Journal of Nuclear Cardiology* published excellent articles pertaining to imaging in patients with cardiovascular disease due to the dedication of the investigators in our field all over the world. In this review, we will summarize a selection of these articles to provide a concise review of the main advancements that have recently occurred in the field and provide the reader with an opportunity to review a wide selection of articles. We will focus on publications dealing with positron emission tomography, computed tomography, and magnetic resonance and hope that you will find this review helpful. (J Nucl Cardiol 2021;28:2100–11.)

Key Words: Heart failure < diseases/processes • Amyloid heart disease < diseases/processes • Sarcoid heart disease < diseases/processes • PET < modalities • MRI < modalities • CT < modalities

INTRODUCTION

The year 2020 has been a tough year for everyone. Yet, despite the COVID-19 pandemic and the endless challenges that followed, research and innovation have not stopped. The determination of scientists has led to more discoveries in the field of nuclear cardiology. It has been a tradition to summarize some of the key articles that were published each year.[1–11] This review is dedicated to the colleagues and loved ones we lost during the pandemic, and to the bright minds whose vigorous and endless efforts and dedication transcended all obstacles to provide us with these amazing papers.

Reprint requests: Fadi G. Hage, MD, MASNC, Division of Cardiovascular Disease, Department of Medicine, University of Alabama at Birmingham, Lyons Harrison Research Building 306, 1900 University BLVD, Birmingham, AL 35294; *fadihage@uab.edu*
1071-3581/$34.00

This review will specifically address articles published in the Journal relating to positron emission tomography (PET), cardiac computed tomography (CT), and cardiac magnetic resonance (CMR).

CORONARY ARTERY DISEASE AND ATHEROSCLEROSIS

Coronary artery disease (CAD) remains a leading cause of morbidity and mortality. The drive to improve diagnostic and prognostic tools through the optimization of current techniques and innovation with new ones is ongoing and seems unstoppable.

Early detection of atherosclerotic plaques is an integral component in the fight against CAD. Inflammation within plaques results in the progression of atherogenesis, development of microcalcification and full-blown calcification, and predicts cardiovascular outcomes.[12,13] Coronary artery calcifications are easily detected on cardiac CT, on CT attenuation correction used with PET imaging, CT chest, and others, and

correlate with early myocardial dysfunction.[14] Similarly, calcifications of non-coronary artery vasculature are equally important since atherogenesis is a systemic process that involves all arterial beds. For instance, calcifications of breast arteries seen on mammogram correlate well with coronary artery calcification and predict mortality.[15]

While CT detects mature calcification, 18F-sodium fluoride (NaF) PET tracer has high affinity for microcalcification within plaques that may not be detected yet with CT and therefore is a promising tool for early detection of atherogenesis. 18F-NaF PET has been used in the detection of early coronary microcalcification; however, the interpretation of the images remains challenging given small size of the coronary arteries and motion artifact.[16] Imaging plaques within the carotid arteries using this tracer is promising. Indeed, Hop H and colleagues compared 23 carotid plaques from stroke patients undergoing surgery (17 culprit, 6 non-culprit). The samples were incubated in 18F-NaF and scanned using microPET.[17] The 18F-NaF uptake was also compared with visualized calcification from microCT scan (Figure 1). 18F-NaF PET imaging showed comparable uptake of tracer between the culprit and non-culprit lesions, and therefore was unable to distinguish between them. The study reaffirms that microcalcification detected with 18F-NaF PET may represent a different and more likely earlier stage in the calcification process than CT, hence inciting further efforts in detecting and imaging early atherogenesis. These new exciting and challenging findings resulted in the paper being awarded the ''Frans J Th Wackers Best Clinical paper.''

There is an increasing role for cardiac CT angiography (CCTA) and hybrid imaging for the diagnosis of CAD. In a systemic review and meta-analysis of 661 original studies (71,823 patients), Biondi-Zoccai et al. showed that non-invasive hybrid imaging tests (sensitivity 87%, specificity 82%) appear superior to anatomic or functional-only tests to diagnose ischemia-provoking coronary lesions (FFR as gold reference), whereas anatomic imaging (sensitivity 95%, specificity 83%) is best to diagnose and/or rule out angiographically significant CAD (invasive coronary angiogram as gold reference).[18]

Myocardial-coronary fusion imaging with PET and CCTA represents a promising concept in hybrid imaging by moving forward with the integration of anatomic and functional imaging for CAD. In a pilot study, Piccinelli et al. performed image fusion techniques to align studies of patients undergoing 13NH3-PET/CT and CCTA. Myocardial blood flow (MBF) was calculated by means of a 1-tissue compartmental model for the standard vascular territories and along patient-specific vessel paths from the base to the apex of the heart. The authors associated a specific myocardial segment to a specific coronary segment (using CCTA for anatomic mapping) and compared the results of PET in the specific volume of interest. Color-coded images were then generated resembling 3-dimensional fractional flow reserve (FFR).[19,20]

Innovative ideas should be validated and optimized in large multicenter studies before routine clinical application. Going forward with the idea of PET/CCTA myocardial-coronary fusion imaging, the dynamic PET/

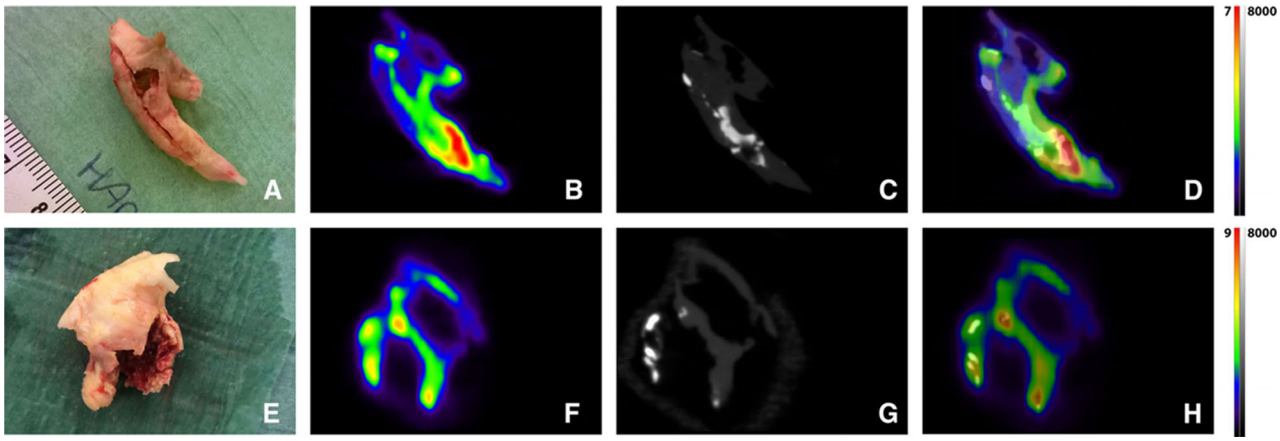

Figure 1. 18F-NaF microPET and microCT images of human carotid plaque. (**A**, **E**) Human carotid plaque after carotid endarterectomy. (**B**, **F**) Sagittal view of ex vivo PET showing a heterogeneous distribution of 18F-NaF uptake with a clear hotspot (red/yellow). (**C**, **G**) Sagittal view of corresponding microCT images. (**D**, **H**) Fused images showing different distributions of microcalcification (18F-NaF PET) and established calcification (microCT). Scale PET images in %Inc/g, scale CT images in HU. Reproduced with permission from Hop et al.[17] (Figure 1, p. 1070).

CTA myocardial blood flow assessment with fused imagery (DEMYSTIFY) study is an observational prospective clinical study that will develop algorithms and software tools to fuse coronary anatomy data obtained from CTA with dynamic PET data to non-invasively measure absolute MBF, myocardial flow reserve, and relative flow reserve across specific coronary lesions. Potential benefits include avoiding unnecessary invasive angiography and angioplasties; guiding revascularization to the culprit vessel; providing a complete 3D color flow coded map of the coronary tree, while avoiding excess radiation and minimizing overall cost.[21]

Vasodilator stress PET myocardial perfusion imaging (MPI) with dynamic acquisition provides the tools to quantify different parameters of absolute MBF, including hyperemic MBF, myocardial flow reserve, and relative flow reserve. In a pooled analysis of 10 studies (2,522 arteries, 1,099 patients), Cho et al. showed that hyperemic MBF had the best sensitivity (85.3%) and relative flow reserve the best specificity (89.7%) for the diagnosis of significant coronary stenosis, both outperforming myocardial flow reserve.[22]

While FFR is routinely obtained on dynamic PET - MPI and recognized as gold standard for detection of ischemia and to appropriately guide therapy, a recent study by Yokota et al. raised some concern regarding vessel-specific high false-positive rates. Indeed, an abnormal FFR was observed in 35.3% of the LAD measurements, compared to 9.8% in the non-LAD measurements ($P = 0.001$) (adjusted odds ratio 5.3, 95% CI 2.2-12.3). Of the abnormal FFR LAD measurements, 70% were non-obstructive on invasive angiography.[23] This discrepancy creates a clinical dilemma, particularly that data have shown improved outcomes with FFR-guided therapy. While the mechanism for such high false-positive rate particularly in the LAD remains unclear, FFR should still be interpreted in the context of MPI and individualized to each patient.[24]

Multivessel CAD is often challenging to detect on MPI where perfusion defects sometimes underestimate the extent of disease. Transient ischemic dilatation, stress-induced decrease in LV ejection fraction, abnormal MBF, among other variables provide additional and complementary prognostic data to traditional perfusion imaging.[25] Mechanical dyssynchrony can also be quantified from gated PET imaging to generate both systolic and diastolic dyssynchrony parameters, and carries incremental prognostic value.[26,27] In a recent study, Van Tosh et al. analyzed PET MPI of 105 patients undergoing evaluation for CAD and identified 15 having multivessel disease confirmed with angiography. Diastolic regional asynchrony outperformed MBF in detecting patients with multivessel disease (area under the curve [AUC] 83% vs. 73%).[28] Despite being a small size study, it sheds the light once more on the importance of mechanical dyssynchrony indices which are easily obtained from gated images, have diagnostic and prognostic value, and should be reported routinely in all studies.

The use of CZT camera in SPECT MPI has been associated with improved image quality, less attenuation artifact, and better performance than traditional cameras, particularly among overweight patients. Whether SPECT MPI with CZT performs similarly to 82Rb-PET imaging is unclear. Hyafil et al. compared the performance of SPECT MPI with CZT to 82Rb-PET in 313 women and overweight patients, using coronary angiography with FFR as the gold standard. The study showed similar specificity, but significantly higher sensitivity for PET to detect high-risk CAD when compared to CZT SPECT (85% vs. 57%, $P < 0.05$) and better overall diagnostic performance (AUC 0.86 vs. 0.75, $P = 0.04$).[29] While attenuation correction and MBF calculation were performed with 82Rb-PET, neither of them was used with SPECT imaging despite the fact that CZT camera has robust attenuation correction and the capability to quantify MBF.[30]

Although cardiac PET imaging provides high diagnostic quality imaging and outperforms SPECT, it remains susceptible to artifact with room for optimization. In particular, increased gastric activity which is seen in 10% of 82Rb-PET MPI often causes inferior attenuation artifact and in extreme cases may lead to inconclusive studies. In an interesting observational study, Alzahrani et al. showed that proton pump inhibitors increased gastric spillover of 82Rb in patients undergoing stress testing.[31] Whether such increase in gastric uptake of 82Rb was associated with clinically significant number of inconclusive or non-diagnostic studies is of interest and unfortunately was not reported in the study. Also, whether proton pump inhibitor might influence image quality with 13NH3-PET and SPECT is unclear. While awaiting further studies to validate these findings, it may be reasonable to advise patient to withhold proton pump inhibitors prior to 82Rb-PET imaging.[32]

Coronary artery plaques may rupture causing acute coronary syndrome. Post acute myocardial infarction, complex inflammatory processes occur resulting in myocardial scarring and ventricular remodeling. In a swine model of ischemia-reperfusion injury and infarction, using 18FDG-PET to image inflammatory and metabolic changes, Xi et al. showed increased FDG uptake in the infarct zone on day 1 and which persisted up to 14 days. The increased FDG uptake correlated with left ventricular (LV) remodeling, reduced ejection fraction, and increased ventricular volumes.[33] The

unexpected persistence of FDG uptake at last 14 days post MI is unclear, but speculated to be due to macrophage infiltration. FDG may not be the optimal tracer for inflammation and may overestimate the signal if physiologic uptake is not adequately suppressed; using specific markers for inflammation and macrophages might provide additional pathophysiological insights on post-MI remodeling.[34]

NON-ISCHEMIC CARDIOMYOPATHY

Amyloidosis

99mTc pyrophosphate bone scan imaging is routinely performed in the imaging and diagnosis of transthyretin cardiac amyloidosis (ATTR-CA).[35] Given the high calcium content of the amyloid fibrils, 18F-NaF PET has been evaluated as a potential imaging modality for ATTR-CA given its high affinity to calcium. Martineau et al. [36] performed MPI with 18NaF PET in 7 subjects with ATTR-CA, 4 with AL-CA, and 4 controls. The target-to-background ratios (TBR) were significantly increased in the ATTR-CA subjects compared to AL-CA and control, while LV standardized uptake values (SUV) were not. TBR cut-off value of 0.89 had a sensitivity/specificity of 75%/100% (AUC 0.91) and outperformed qualitative interpretation (SN/SP 57%/100%). Despite high specificity, the low TBR ratios indicate poor myocardial signal resulting in reduced sensitivity that needs further improvement before clinical use.

The role of SPECT imaging in the diagnosis of AL-CA remains limited. 11C-Pittsburgh B (PIB) is a newly proposed tracer used in PET imaging of CA that allows direct imaging of amyloid fibrils, and capable to imaging both AL and ATTR. The 11C-PIB uptake pharmacodynamics in CA were recently explained and quantified using an irreversible two-tissue model that successfully discriminated patients with CA and controls using SUV and region of interest.[37] Not only is 11C-PIB useful in the diagnosis of CA, but also recently shown to have prognostic value as shown in small size pilot study comparing 11C-PIB PET/CT with 99mTc-aprotinin scintigraphy in subjects with CA with serial imaging over a period of 2 months.[38] Despite the small size sample and potential false-positive results from Tc-aprotinin, the results are ''certainly provocative and represent early efforts to identify PET imaging techniques that offer prognostic data in patients with CA and thus the ability to potentially guide management decisions.''[39] While the clinical use of 11C-PIB might be challenging given its short half-life and the need for an on-site cyclotron, 18F-florbetapir (FDA-approved brain imaging agent) is an emerging PET tracer which may circumvent some of these limitations and potentially prove to be useful in the evolving landscape of nuclear imaging in CA.

In a meta-analysis of six studies (39 subjects with AL, 30 with ATTR), using 11C-PIB (four studies) and 18F-florbetapir (two studies), the pooled sensitivity, specificity, positive LR, and negative LR of these two agents were 0.95, 0.98, 10.1, and 0.1, respectively. Furthermore, the semiquantitative parameters of amyloid PET showed significantly higher values for CA patients than those for controls, and could discriminate AL versus ATTR ($P < 0.001$), hence offering a potential advantage over SPECT.[40] Contrary to bone-seeking agents used with SPECT imaging, PET radiotracers seem to be the first to specifically image AL-CA, with a high TBR, hence minimizing the need for further biopsy confirmation, and potentially quantifying amyloid burden and response to therapy.[41] While these PET agents are approved mainly for brain imaging in many countries, their clinical use should be expanded to cardiac imaging.

Hypertrophic Cardiomyopathy

Patients with hypertrophic cardiomyopathy are not uncommonly referred for stress imaging for symptoms of angina, which often turns out to be secondary to microvascular dysfunction. Yalçin et al. evaluated 108 patients with hypertrophic cardiomyopathy undergoing both vasodilator stress PET and exercise stress echocardiogram.[42] Vasodilator-induced transient LV cavity dilation (ratio > 1.13 stress/rest) was observed in 51% of patients; this subgroup had lower stress PET-EF, reduced myocardial blood flow, increased LV mass, and lower global longitudinal strain, which may represent microvascular dysfunction. However, on exercise stress echocardiogram, only one patient had LV cavity dilation, while the EF at peak exercise increased in all patients. Differences in the cardiac effects of exercise and vasodilators and timing of stress-image acquisition could explain the discordances between PET and echocardiography. Still vasodilator stress PET imaging may potential be a useful tool and reflect a greater sensitivity and ability to detect early myopathy and microvascular dysfunction.

Sarcoidosis

Sarcoidosis is an inflammatory cardiomyopathy associated with arrhythmia, sudden cardiac death, and heart failure.[43] 18FDG-PET/CT plays a significant role in the diagnosis of cardiac sarcoidosis. Indeed, in a recent meta-analysis of 17 studies with 891 patients, the pooled sensitivity, specificity, positive LR, and negative

LR were 84%, 83%, 4.9, and 0.2, respectively. Furthermore, the pooled diagnostic odds ratio was 27 (95% CI 14-55) with AUC of 0.90. The moderate sensitivity and specificity of FDG-PET imaging is encouraging and could be further enhanced using combined myocardial perfusion imaging data.[44]

Both FDG uptake on PET imaging [45] (surrogate of active inflammation) and late gadolinium enhancement on CMR [43] (surrogate for scar) are predictive of major cardiovascular adverse events. However, the level of FDG uptake that predicts outcomes is not well established. Among 67 patients with cardiac sarcoidosis undergoing 18F-FDG-PET/CT MPI, maximal and mean SUV uptake particularly at the basal septum were predictors of composite endpoint (ventricular tachycardia, AICD placement, complete heart block, pacemaker placement, atrial fibrillation, heart failure, and cardiac-related hospital admissions) after a mean follow-up of 3 years, and with corresponding odds ratios of 1.068 ($P = 0.002$) and 1.059 ($P = 0.023$), respectively.[46] Hybrid PET/CMR is an alternative modality that is gaining momentum in imaging cardiac sarcoidosis, and was shown in a small size study to provide similar diagnostic data for 18F-FDG uptake compared to PET/CT.[47]

A successful 18FDG/PET imaging of cardiac sarcoidosis necessitates adequate suppression of physiologic FDG uptake, which in turn is highly dependent on strict diet preparation prior to the study. Different protocols have been adopted with variability in the duration of fasting, carbohydrate-restricted diets, and others. Atterton-Evans et al. conducted a systematic review of 13 studies (11 human, 2 animal) and showed significant variations in measures used, dietary prescriptions, and fasting times; hence, the authors were unable to perform adequate comparison to provide unified recommendation.[48] While centers adopt their own protocols, many are currently performing low-carb, high-fat diet; 18 hours of fasting (12 hours for diabetic), and heparin injection to adequately suppress physiologic FDG uptake.[49] The optimal protocol is yet to be confirmed in a randomized trial.

Patients with cardiac sarcoidosis often have extra-cardiac involvement. In a pilot study of 33 patients with FDG uptake in the left ventricle consistent with cardiac sarcoidosis, Tuominen et al. found that 12/33 had right ventricular uptake, and 16/33 had extra-cardiac uptake that was associated with higher SUV max values in the myocardium.[50] In addition, 10/12 patients with both ventricular uptake had extra-cardiac involvement as opposed to 6/21 with isolated left ventricular uptake. Biventricular involvement and extra-cardiac FDG uptake were predictive of a biopsy indicative of sarcoidosis. As stated in an editorial by Tahara et al. this is ''noteworthy because it is better to get a histologic proof of granulomatous inflammation for accurately diagnosing CS, which has important prognostic and therapeutic implications to the individual involved.''[51]

Chemotherapy Induced

Cardiac oncology has significantly grown to become its own specialty.[52] Doxorubicin is the cornerstone chemotherapy agent in patients with lymphoma, but often associated with dose-related irreversible myocardial necrosis that results in cardiomyopathy and heart failure. Indeed, doxorubicin may result in increased myocardial oxidative stress, resulting into inflammation and ultimately cellular death and scarring. In a pilot animal study, Baucknehet et al. demonstrated directed correlation between Doxorubicin-induced myocardial oxidative stress (ascertained with biochemical, histological, and immunohistochemical analyses) and FDG uptake, therefore supporting the potential role of 18FDG-PET imaging to detect early anthracycline-induced cardiomyopathy.[53] The identification of patients at highest risk of such cardiomyopathy is key to reduce hospitalization for heart failure and cardiovascular-related death. In a recent study, Laursen et al. performed rest and vasodilator stress 82Rb-PET MPI for 54 patients with lymphoma pre and post first dose of doxorubicin. Coronary microvascular dysfunction was defined as worsening of myocardial perfusion reserve with a drop greater than 20% on serial imaging (post-pre).[54] Indeed, myocardial flow reserve represents a sensitive marker of vascular function and therefore a potentially marker of early myocardial injury. The authors identified 41 patients who developed microvascular coronary dysfunction post doxorubicin, and considered them as potentially higher risk for developing cardiomyopathy.[54] While advanced age was the only variable distinguishing patients with and without drop in perfusion reserve, it remains unclear whether this new microvascular dysfunction is an independent predictor of anthracycline-induced cardiomyopathy after adjusting for age and other key variables.[55]

Anthracycline and trastuzumab are commonly used in patients with breast cancer. Surveillance with echocardiography, particularly global longitudinal strain, is key for early detection of cardiomyopathy and initiating early treatment with beta blockers and angiotensin-converting enzyme inhibitors or changing chemotherapy agents. Using FDG-PET imaging to detect early chemotherapy-induced myocardial inflammation and cellular damage, Kim et al. showed that the presence of right ventricular wall uptake and/or increase of SUV of right ventricular wall on post-therapy were

associated with early cardiotoxicity among 121 breast cancer patients who underwent anthracycline or trastuzumab [56] (Figure 2). Unlike anthracycline, trastuzumab induced cellular apoptosis rather than inflammation and necrosis; it remains to be seen in larger studies whether these different pathways of chemotherapy-induced cardiomyopathy would result in different FDG uptake patterns, and would influence the sensitivity of the PET imaging.

INFECTIOUS DISEASE

Chagas's disease in an infectious cardiomyopathy associated with microvascular dysfunction, autonomic denervation, and myocardial fibrosis that lead to ventricular arrhythmia, heart failure, and sudden death. Barizon et al. performed an interesting study of 13 patients with confirmed Chagas disease that underwent 123I-MIBG SPECT, rest-stress 99mTc-Sestamibi, and cardiac MRI with late gadolinium enhancement. The areas of scarring and autonomic dysfunction correlated well between the different imaging modalities.[57] Given the superiority of PET and better ability quantify coronary flow reserve and detect inflammation, a PET/MR hybrid imaging seems to be a comprehensive modality in patients with Chagas disease. For the avid readers interested in more information about Chagas disease, we would highly recommend the following editorial by Vellasco et al.[58]

Infective endocarditis is a devastating infectious disease that is sometimes difficult to diagnose and requires multi-modality imaging for confirmation. In an observational single-center study, Gomes et al. prospectively enrolled 176 patients with suspected endocarditis (native/devices) and compared imaging techniques head to head in 46 patients that underwent echocardiogram, CT, and FDG-PET. Echocardiography, CT, and FDG-PET provided relevant complementary diagnostic information. In particular, CT performed best in the assessment of abscesses and ventricular assist device infection, while FDG-PET performed best in the assessment of cardiac device infection, extra-cardiac infectious foci, and alternative diagnoses.[59] It is important to note that the ''patient management in the authors'

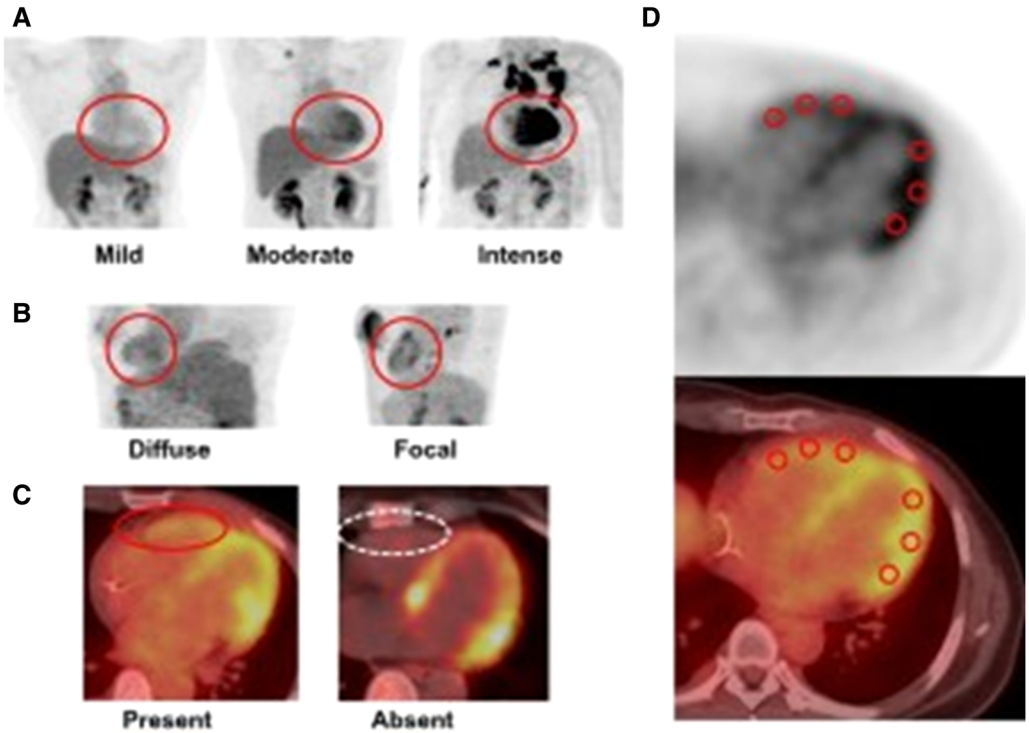

Figure 2. Association between increased 18FDG uptake in the right ventricle with diffuse left ventricular involvement as a marker of early chemotherapy-induced cardiotoxicity in patients with breast cancer. Anthracycline and trastuzumab were associated with various patterns of 18FDG uptake on PET imaging in the left and right ventricles. Patients with right ventricular involvement were more likely to have diffuse left ventricular involvement and subsequently more likely to have chemotherapy associated with cardiotoxicity. Reproduced with permission from Kim et al. [56] (Figure 1).

hospital did not comply with their own protocol in 31% of cases.'' Also, the complexity of the algorithm and the requirements/skills needed to perform all imaging modalities represent challenges, especially for non-tertiary referral centers.[60]

ATRIAL FIBRILLATION

Increased left atrial sympathetic activity is a known precursor for atrial fibrillation. There has been increasing interest in imaging the left atrium sympathetic activity using 123I-MIBG.[61] Inflammation also predisposes to such arrhythmia. Indeed, a recent retrospective study evaluated 48 patients with atrial fibrillation (32 persistent, 16 paroxysmal) undergoing 18FDG-PET imaging. Seventeen patients, all with persistent atrial fibrillation, had increased atrial FDG uptake, particularly in the right atrium, and 11 patients had increased uptake in the left atrial appendage. Both right atrial and appendage activities correlated with increased activity in epicardial adipose tissue.[62] This technique may identify subgroup of patients where inflammation may play a role in the pathogenesis of atrial fibrillation. The fact that mainly patients with persistent atrial fibrillation had increased FDG uptake is in agreement with the paper by Ghannam et al. that showed high correlation between atrial fibrillation burden and left atrial remodeling (inflammation and scar)[63] (Figure 3). Still, the small number of patients, suboptimal characterization of atrial fibrillation (duration ranging from 1 to 66 months), and variability in FDG suppression with high residual physiologic uptake in the ventricles are several limitations for the study of Xie et al. as pointed out in two accompanying editorials.[64,65] Partial volume averaging of a thin left atrium, increase in atrial wall thickness in patients with left atrial overload tend to overestimate FDG uptake. Also, gated artifact during PET image acquisition due to heart rate fluctuation is another source of error.[66] Many of these challenges were also faced and overcome with late gadolinium enhancement cardiac MRI assessment of left atrial scar. PET, on the other hand, has an advantage of being able to image easily patients with devices. Ideally, PET/CMR hybrid imaging of left atrial remodeling would seem to be the ideal comprehensive modality.

EXTRA CARDIAC IMAGING

Non-alcoholic Fatty Liver

Non-alcoholic fatty liver disease (NAFLD) is recognized as an independent predictor of cardiovascular disease. The majority of patients with NAFLD die from cardiovascular disease and only 5% from liver disease.[67] In a pilot study of 743 asymptomatic subjects (201 with NAFLD, 542 without NAFLD), Tung et al. found a strong association between NAFLD and decreased myocardial glucose uptake (assessed with 18FDG-PET and quantified using SUVmax) that persisted after multivariate adjustment and correlated with increased LV filling pressures, a reflection of early diastolic dysfunction.[68] Previous work published by Lee and colleagues showed significant correlation between NAFLD and vascular inflammation with 18F-FDG-PET in the carotid arteries [69]; however, the present study is the first to elicit through imaging the correlation between NAFLD and potential cardiac metabolic abnormalities. ''The reasons for alterations of the biochemical processes of myocardial glucose uptake in patients with NAFLD is not clear, but probably is the result of several complex biochemical processes involving genetic factors, atherosclerosis, inflammatory cytokines, insulin resistance, and other alterations in biochemistry of glucose and fatty acid metabolism,'' as pointed out by Gullberg et al. in an accompanying editorial.[70]

Incidental Findings of Cardiac CT and CT Attenuation Images

Extra-cardiac incidental findings on cardiac CT or CT attenuation images are common and associated with all-cause and cancer-specific mortality.[71] Using data from randomized controlled trial of patients with chest pain (cardiac CT vs. MPI), Goldman et al. found no extra-cardiac incidental findings in the MPI arm that served as a control versus 386 incidental findings among 187 cardiac CT studies. Patients in the cardiac CT group underwent subsequently more inpatient testing ($P = 0.042$) and outpatient CT chest in the year following admission (14% vs. 3%, $P = 0.029$).[72] Therefore, incidental findings often result in more downstream testing that will incur higher cost and burden to the healthcare system.

Bone Density and Cardiovascular Outcomes

Reduced bone mineral density has been shown in few studies to be associated with heart failure, although the pathophysiology remains unclear.[73] Fietcher et al. evaluated bone mineral density obtained from CT attenuation images of 491 patients (mean age 65 years, 32% women) undergoing 13NH3-PET/CT imaging for evaluation of CAD. After a median follow-up of 4.3 years, patients with reduced bone density ($\leq$ 100 Hounsfield units) had significantly worse outcomes (log rank $P = 0.037$). Furthermore, reduced bone mineral density was an independent predictor of cardiovascular

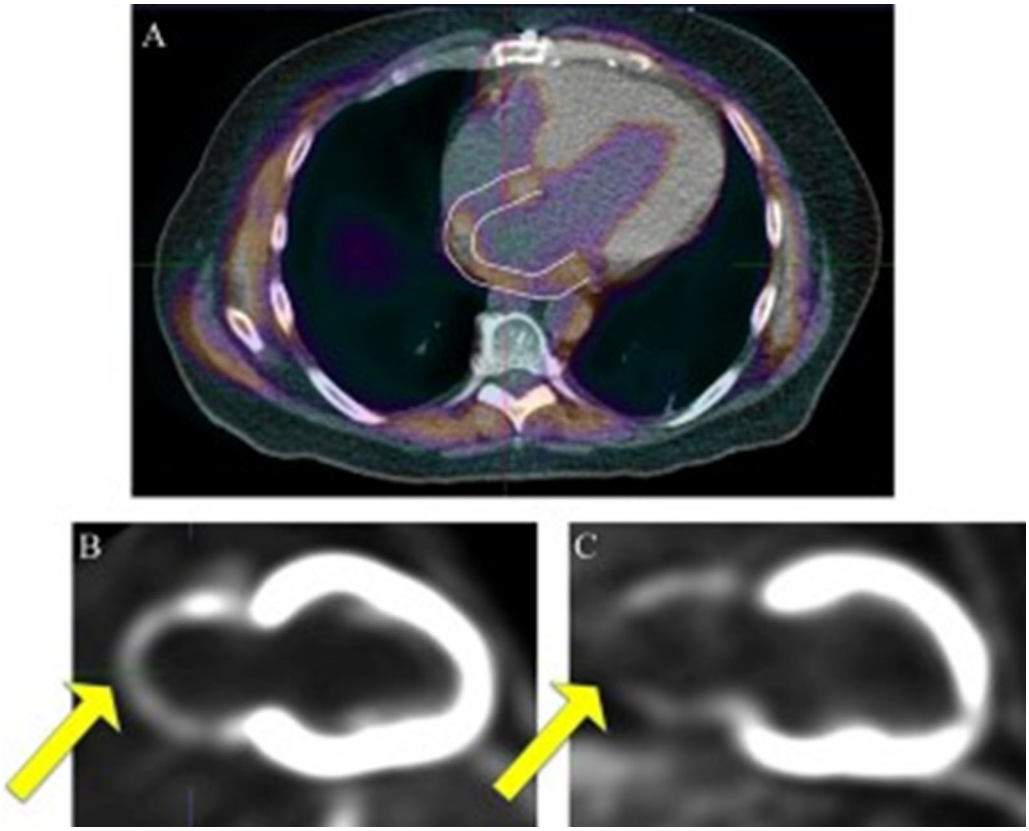

Figure 3. 18FDG uptake on PET imaging in patients with atrial fibrillation. The figure illustrates different patterns of left atrial remodeling and uptake of 18FDG in patients with atrial fibrillation using PET. Reproduced with permission from Ghannam et al. [63] (Figure 1).

events in men but not in women (*P* for interaction = 0.007).[74] Therefore, CT attenuation correction imaging obtained from PET MPI are useful not only to assess for coronary artery calcification, but also for reduced bone mineral density, particularly in men, as the data seem to have incremental prognostic value and is readily available for analysis.

TECHNICAL CORNER

Quantitative perfusion and coronary flow capacity with PET MPI may be overestimated by 50-150% if correction of partial volume loss due is not properly performed.[75] Similarly, accurate and reproducible arterial input function is essential as it may alter the optimal guidance of intervention in at least 7% of patients.[76] Motion artifact is another pitfall in PET imaging that may impact accurate MBF quantification with 82Rb-PET. Although motion correction can be performed manually, this might introduce a source of variability, particularly when serial imaging and comparison are needed. Poitrasson-Rivière et al. showed in a randomized blinded trial that automated motion correction significantly decreased inter-user variability and reduced processing time.[77]

PET/CMR hybrid imaging is a powerful modality that takes advantages of two complementary techniques, and is more commonly utilized. However, it is technically more challenging than other modalities, particularly with the multiple associated artifacts in the MR-based attenuation correction maps. In a recent study that was awarded the ''William Strauss Best Technical paper,'' Lassen M and colleagues performed 13NH3-PET/MR in 20 patients with ischemic cardiomyopathy, utilizing standard DIXON-attenuation correction.[78] The average respiratory misalignment was 7 mm and observed in 90% of patients. Furthermore, susceptibility artifacts were observed in half of the patients along with substantial changes in lung volumes on attenuation correction maps, and almost a third had tissue inversion artifact. All of these resulted in 15% false-positive rate (Figure 4).[78] Therefore, in PET/CMR hybrid imaging studies, standard DIXON-attenuation correction maps must be examined carefully for artifacts and

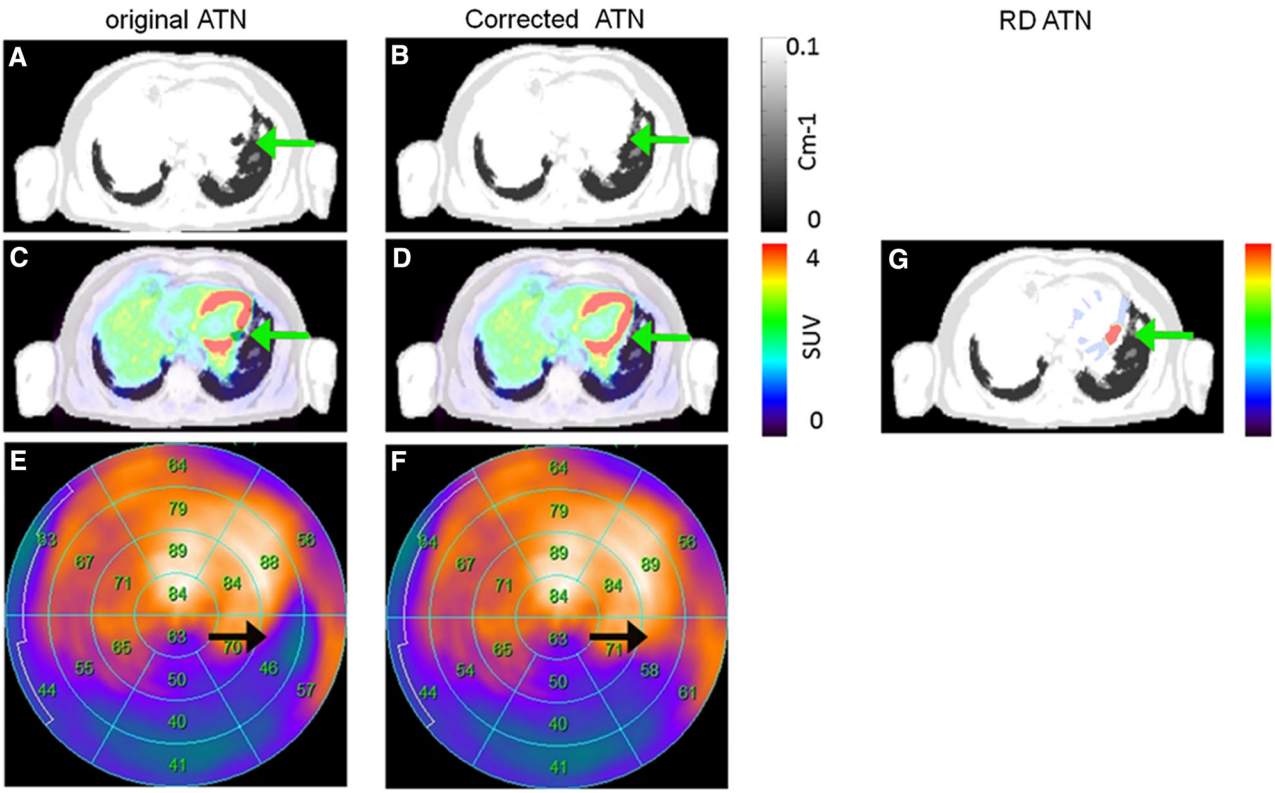

Figure 4. Attenuation (ATN) correction with PET/CMR hybrid imaging. Hybrid PET/CMR images showing susceptibility artifact on CMR images caused by a stent resulting in an artifact in the left circumflex artery territory in the original AC map (**A**, arrow) that was interpreted incorrectly as perfusion defect. Correction of the susceptibility artifact (**B**) changed the interpretation from reduced metabolism to normal metabolism (**C**–**F**, arrows). The susceptibility artifact accounted for relative differences of more than 10% in the affected region (**G**). Reproduced with permission from Lassen et al. [78] (Figure 5, p. 1114).

misalignment effects to avoid misinterpretation of biased perfusion and metabolism readings from the PET data.

The standard Dixon-based attenuation correction in PET/CMR segments only the air, lung, fat, and soft-tissues (4 class), while neglecting the highly attenuating bone tissues which may affect quantification in bones and adjacent vessels. Utilizing the distinctively high bone uptake rate constant Ki expected from 18F-NaF to segment bones from PET data, Karakatsanis et al. showed that 5-class hybrid PET/MR-driven attenuation correction (compared to 4 class) resulted in 18% higher TBR at carotid bifurcation with 18F-NaF and similarly with 18FDG-PET. Results were independent of history of prior CAD.[79]

Quantitative parameters are derived from perfusion and gated imaging using one of the commercially available software packages. With SPECT imaging, our group have shown significant differences between three softwares in measuring perfusion defect size, LV function, and more importantly quantifying defect size.[80,81] Similar study was performed with 82Rb-PET measuring LV volumes, mass, and EF using different software packages; while measurement were reproducible within each software, the concordance between software was poor, hence necessitating the use of same software particularly with serial imaging.[82] Similarly, poor agreement with reversible defects, global stress MBF and MFR, and regionally dependent discrepancies were noted among 3 softwares used to process dynamic data from 13NH3-PET.[83] Therefore, each PET facility should strive for consistency not only in the choice of positron-emitting radiotracer, protocols, and remaining steps in the processing of desired quantitative parameters, but also in their software package for optimal patient care.[84]

References

1. AlJaroudi WA, Hage FG. Review of cardiovascular imaging in the Journal of Nuclear Cardiology 2019: Positron emission tomography, computed tomography and magnetic resonance. J Nucl Cardiol. 2020;27:921–30.

2. Hage FG, AlJaroudi WA. Review of cardiovascular imaging in the Journal of Nuclear Cardiology 2019: Single-photon emission computed tomography. J Nucl Cardiol. 2020;27:1171–9.
3. AlJaroudi WA, Hage FG. Review of cardiovascular imaging in the Journal of Nuclear Cardiology 2018. Part 1 of 2: Positron emission tomography, computed tomography, and magnetic resonance. J Nucl Cardiol. 2018;2019:524–35.
4. Hage FG, AlJaroudi WA. Review of cardiovascular imaging in the Journal of Nuclear Cardiology in 2017. Part 2 of 2: Myocardial perfusion imaging. J Nucl Cardiol. 2017;2018:1390–9.
5. AlJaroudi WA, Hage FG. Review of cardiovascular imaging in the Journal of Nuclear Cardiology 2017. Part 1 of 2: Positron emission tomography, computed tomography, and magnetic resonance. J Nucl Cardiol. 2018;25:320–30.
6. Hage FG, AlJaroudi WA. Review of cardiovascular imaging in the journal of nuclear cardiology in 2016: Part 2 of 2-myocardial perfusion imaging. J Nucl Cardiol. 2017;24:1190–9.
7. AlJaroudi W, Hage FG. Review of Cardiovascular Imaging in the Journal of Nuclear Cardiology in 2016. Part 1 of 2: Positron emission tomography, computed tomography and magnetic resonance. J Nucl Cardiol. 2017;24:649–56.
8. Hage FG, AlJaroudi WA. Review of Cardiovascular Imaging in the Journal of Nuclear Cardiology in 2015-Part 2 of 2: Myocardial perfusion imaging. J Nucl Cardiol. 2016;23:493–8.
9. AlJaroudi WA, Hage FG. Review of cardiovascular imaging in the journal of nuclear cardiology in 2015. Part 1 of 2: Plaque imaging, positron emission tomography, computed tomography, and magnetic resonance. J Nucl Cardiol. 2016;23:122–30.
10. Hage FG, AlJaroudi WA. Review of cardiovascular imaging in The Journal of Nuclear Cardiology in 2014: Part 2 of 2: Myocardial perfusion imaging. J Nucl Cardiol. 2015;22:714–9.
11. AlJaroudi WA, Hage FG. Review of cardiovascular imaging in The Journal of Nuclear Cardiology in 2014: Part 1 of 2: Positron emission tomography, computed tomography, and neuronal imaging. J Nucl Cardiol. 2015;22:507–12.
12. Rudd JH, Warburton EA, Fryer TD, Jones HA, Clark JC, Antoun N, et al. Imaging atherosclerotic plaque inflammation with [18F]-fluorodeoxyglucose positron emission tomography. Circulation. 2002;105:2708–11.
13. Sadeghi MM. (18)F-FDG PET and vascular inflammation: time to refine the paradigm? J Nucl Cardiol. 2015;22:319–24.
14. Mansour MJ, Chammas E, Hamoui O, Honeine W, AlJaroudi W. Association between left ventricular diastolic dysfunction and subclinical coronary artery calcification. Echocardiography. 2020;37:253–9.
15. Bui QM, Daniels LB. A review of the role of breast arterial calcification for cardiovascular risk stratification in women. Circulation. 2019;139:1094–101.
16. McKenney-Drake ML, Territo PR, Salavati A, Houshmand S, Persohn S, Liang Y, et al. (18)F-NaF PET imaging of early coronary artery calcification. JACC Cardiovasc Imaging. 2016;9:627–8.
17. Hop H, de Boer SA, Reijrink M, Kamphuisen PW, de Borst MH, Pol RA, et al. (18)F-sodium fluoride positron emission tomography assessed microcalcifications in culprit and non-culprit human carotid plaques. J Nucl Cardiol. 2019;26:1064–75.
18. Biondi-Zoccai G, Versaci F, Iskandrian AE, Schillaci O, Nudi A, Frati G, et al. Umbrella review and multivariate meta-analysis of diagnostic test accuracy studies on hybrid non-invasive imaging for coronary artery disease. J Nucl Cardiol. 2020;27:1744–55.
19. Piccinelli M, Cho SG, Garcia EV, Alexanderson E, Lee JM, Cooke CD, et al. Vessel-specific quantification of absolute myocardial blood flow, myocardial flow reserve and relative flow reserve by means of fused dynamic (13)NH(3) PET and CCTA: Ranges in a low-risk population and abnormality criteria. J Nucl Cardiol. 2020;27:1756–69.
20. Nudi F, Biondi-Zoccai G, Di Belardino N, Nudi A, Schillaci O. Myocardial-coronary fusion imaging with positron emission tomography and computed tomography: Benchmarking and slingshotting. J Nucl Cardiol. 2020;27:1770–3.
21. AlBadri A, Piccinelli M, Cho SG, Lee JM, Jaber W, De Cecco CN, et al. Rationale and design of the quantification of myocardial blood flow using dynamic PET/CTA-fused imagery (DEMYSTIFY) to determine physiological significance of specific coronary lesions. J Nucl Cardiol. 2020;27:1030–9.
22. Cho SG, Lee SJ, Na MH, Choi YY, Bom HH. Comparison of diagnostic accuracy of PET-derived myocardial blood flow parameters: A meta-analysis. J Nucl Cardiol. 2018;27:1955–66.
23. Yokota S, Borren NM, Ottervanger JP, Mouden M, Timmer JR, Knollema S, et al. Does fractional flow reserve overestimate severity of LAD lesions? J Nucl Cardiol. 2020;27:1306–13.
24. Benz DC, Giannopoulos AA. Fractional flow reserve as the standard of reference: All that glistens is not gold. J Nucl Cardiol. 2020;27:1314–6.
25. Bajaj NS, Singh S, Farag A, El-Hajj S, Heo J, Iskandrian AE, et al. The prognostic value of non-perfusion variables obtained during vasodilator stress myocardial perfusion imaging. J Nucl Cardiol. 2016;23:390–413.
26. AlJaroudi W, Alraies MC, Menon V, Brunken RC, Cerqueira MD, Jaber WA. Predictors and incremental prognostic value of left ventricular mechanical dyssynchrony response during stress-gated positron emission tomography in patients with ischemic cardiomyopathy. J Nucl Cardiol. 2012;19:958–69.
27. AlJaroudi W, Alraies MC, DiFilippo F, Brunken RC, Cerqueira MD, Jaber WA. Effect of stress testing on left ventricular mechanical synchrony by phase analysis of gated positron emission tomography in patients with normal myocardial perfusion. Eur J Nucl Med Mol Imaging. 2012;39:665–72.
28. Van Tosh A, Votaw JR, David Cooke C, Cao JJ, Palestro CJ, Nichols KJ. Relationship of (82)Rb PET territorial myocardial asynchrony to arterial stenosis. J Nucl Cardiol. 2020;27:575–88.
29. Hyafil F, Chequer R, Sorbets E, Estellat C, Ducrocq G, Rouzet F, et al. Head-to-head comparison of the diagnostic performances of Rubidium-PET and SPECT with CZT camera for the detection of myocardial ischemia in a population of women and overweight individuals. J Nucl Cardiol. 2020;27:755–68.
30. Grossman GB. Myocardial perfusion imaging in overweight patients and women: Is it CZT good enough? J Nucl Cardiol. 2020;27:769–73.
31. Alzahrani AH, Arasaratnam P, Massalha S, Alenazy A, Lee A, Clarkin O, et al. Effect of proton pump inhibitors on Rubidium-82 gastric uptake using positron emission tomography myocardial perfusion imaging. J Nucl Cardiol. 2020;27:1443–51.
32. Al-Mallah MH. Should patients hold proton pump inhibitors prior to (82)Rubidium positron emission tomography myocardial perfusion imaging? J Nucl Cardiol. 2020;27:1452–5.
33. Xi XY, Zhang F, Wang J, Gao W, Tian Y, Xu H, et al. Functional significance of post-myocardial infarction inflammation evaluated by (18)F-fluorodeoxyglucose imaging in swine model. J Nucl Cardiol. 2020;27:519–31.
34. Miller EJ. Complex cellular physiology underlies the use of FDG-PET imaging in investigating post-infarction remodeling. J Nucl Cardiol. 2020;27:532–3.
35. Aljaroudi WA, Desai MY, Tang WH, Phelan D, Cerqueira MD, Jaber WA. Role of imaging in the diagnosis and management of patients with cardiac amyloidosis: state of the art review and focus on emerging nuclear techniques. J Nucl Cardiol. 2014;21:271–83.

36. Martineau P, Finnerty V, Giraldeau G, Authier S, Harel F, Pelletier-Galarneau M. Examining the sensitivity of 18F-NaF PET for the imaging of cardiac amyloidosis. J Nucl Cardiol. 2019;28:209–18.
37. Kero T, Sörensen J, Antoni G, Wilking H, Carlson K, Vedin O, et al. Quantification of (11)C-PIB kinetics in cardiac amyloidosis. J Nucl Cardiol. 2020;27:774–84.
38. Minamimoto R, Awaya T, Iwama K, Hotta M, Nakajima K, Hirai R, et al. Significance of (11)C-PIB PET/CT in cardiac amyloidosis compared with (99 m)Tc-aprotinin scintigraphy: A pilot study. J Nucl Cardiol. 2020;27:202–9.
39. Promislow SJ, Ruddy TD. The evolving landscape of nuclear imaging in cardiac amyloidosis. J Nucl Cardiol. 2020;27:210–4.
40. Kim YJ, Ha S, Kim YI. Cardiac amyloidosis imaging with amyloid positron emission tomography: A systematic review and meta-analysis. J Nucl Cardiol. 2020;27:123–32.
41. Giorgetti A, Genovesi D, Emdin M. Cardiac amyloidosis: The starched heart. J Nucl Cardiol. 2020;27:133–6.
42. Lu DY, Yalçin H, Sivalokanathan S, Greenland GV, Vasquez N, Yalçin F, et al. Higher incidence of vasodilator-induced left ventricular cavity dilation by PET when compared to treadmill exercise-ECHO in hypertrophic cardiomyopathy. J Nucl Cardiol. 2018;14:10212573.
43. Patel MR, Cawley PJ, Heitner JF, Klem I, Parker MA, Jaroudi WA, et al. Detection of myocardial damage in patients with sarcoidosis. Circulation. 2009;120:1969–77.
44. Kim SJ, Pak K, Kim K. Diagnostic performance of F-18 FDG PET for detection of cardiac sarcoidosis; A systematic review and meta-analysis. J Nucl Cardiol. 2019;27:2103–15.
45. Sperry BW, Tamarappoo BK, Oldan JD, Javed O, Culver DA, Brunken R, et al. Prognostic impact of extent, severity, and heterogeneity of abnormalities on (18)F-FDG PET scans for suspected cardiac sarcoidosis. JACC Cardiovasc Imaging. 2018;11:336–45.
46. Flores RJ, Flaherty KR, Jin Z, Bokhari S. The prognostic value of quantitating and localizing F-18 FDG uptake in cardiac sarcoidosis. J Nucl Cardiol. 2018;27:2003–10.
47. Wisenberg G, Thiessen JD, Pavlovsky W, Butler J, Wilk B, Prato FS. Same day comparison of PET/CT and PET/MR in patients with cardiac sarcoidosis. J Nucl Cardiol. 2019;27:2118–29.
48. Atterton-Evans V, Turner J, Vivanti A, Robertson T. Variances of dietary preparation for suppression of physiological (18)F-FDG myocardial uptake in the presence of cardiac sarcoidosis: A systematic review. J Nucl Cardiol. 2020;27:481–9.
49. Schwartz RG, Malhotra S. Optimizing cardiac sarcoid imaging with FDG PET: Lessons from studies of physiologic regulation of myocardial fuel substrate utilization. J Nucl Cardiol. 2020;27:490–3.
50. Tuominen H, Haarala A, Tikkakoski A, Kähönen M, Nikus K, Sipilä K. 18-FDG-PET in a patient cohort suspected for cardiac sarcoidosis: Right ventricular uptake is associated with pathological uptake in mediastinal lymph nodes. J Nucl Cardiol. 2020;27:109–17.
51. Tahara N, Bekki M, Sugiyama Y, Tahara A, Fukumoto Y. Importance of extracardiac FDG uptake to diagnose cardiac sarcoidosis. J Nucl Cardiol. 2020;27:118–22.
52. Chen-Scarabelli C, McRee C, Leesar MA, Hage FG, Scarabelli TM. Comprehensive review on cardio-oncology: Role of multimodality imaging. J Nucl Cardiol. 2017;24:906–35.
53. Bauckneht M, Pastorino F, Castellani P, Cossu V, Orengo AM, Piccioli P, et al. Increased myocardial (18)F-FDG uptake as a marker of Doxorubicin-induced oxidative stress. J Nucl Cardiol. 2019;27:2183–94.
54. Laursen AH, Elming MB, Ripa RS, Hasbak P, Kjær A, Køber L, et al. Rubidium-82 positron emission tomography for detection of acute doxorubicin-induced cardiac effects in lymphoma patients. J Nucl Cardiol. 2020;27:1698–707.
55. Ziadi MC, de Kemp R, Beanlands RSB, Small GR. Looking for trouble: Reduced myocardial flow reserve following anthracyclines. J Nucl Cardiol. 2020;27:1708–13.
56. Kim J, Cho SG, Kang SR, Yoo SW, Kwon SY, Min JJ, et al. Association between FDG uptake in the right ventricular myocardium and cancer therapy-induced cardiotoxicity. J Nucl Cardiol. 2019;27:2154–63.
57. Barizon GC, Simões MV, Schmidt A, Gadioli LP, Murta Junior LO. Relationship between microvascular changes, autonomic denervation, and myocardial fibrosis in Chagas cardiomyopathy: Evaluation by MRI and SPECT imaging. J Nucl Cardiol. 2020;27:434–44.
58. Velasco A, Morillo CA. Chagas heart disease: A contemporary review. J Nucl Cardiol. 2020;27:445–51.
59. Gomes A, van Geel PP, Santing M, Prakken NHJ, Ruis ML, van Assen S, et al. Imaging infective endocarditis: Adherence to a diagnostic flowchart and direct comparison of imaging techniques. J Nucl Cardiol. 2020;27:592–608.
60. Pizzi MN, Fernández-Hidalgo N. Optimizing the diagnostic workup of infective endocarditis: An urgent need for studies focused on defining the decision-making process. J Nucl Cardiol. 2020;27:609–11.
61. Kawasaki M, Yamada T, Furukawa Y, Morita T, Tamaki S, Kida H, et al. Are cardiac sympathetic nerve activity and epicardial adipose tissue associated with atrial fibrillation recurrence after catheter ablation in patients without heart failure? Int J Cardiol. 2020;303:41–8.
62. Xie B, Chen BX, Wu JY, Liu X, Yang MF. Factors relevant to atrial (18)F-fluorodeoxyglucose uptake in atrial fibrillation. J Nucl Cardiol. 2020;27:1501–12.
63. Ghannam M, Yun HJ, Ficaro EP, Ghanbari H, Lazarus JJ, Konerman M, et al. Multiparametric assessment of left atrial remodeling using (18)F-FDG PET/CT cardiac imaging: A pilot study. J Nucl Cardiol. 2020;27:1547–62.
64. Chung MK, Wass SY, Cerqueira M. Imaging and atrial fibrillation: A new paradigm for precision targeting of AF? J Nucl Cardiol. 2020;27:1513–6.
65. Verberne HJ. Atrial (18)F-FDG uptake is related to permanent atrial fibrillation: Will substrate-based patient selection improve outcome? J Nucl Cardiol. 2020;27:1517–20.
66. Naya M, Manabe O, Tamaki N. New trials for assessment of left atrial dysfunction by FDG-PET. J Nucl Cardiol. 2020;27:1563–5.
67. Eslam M, Valenti L, Romeo S. Genetics and epigenetics of NAFLD and NASH: Clinical impact. J Hepatol. 2018;68:268–79.
68. Tang K, Zheng X, Lin J, Zheng M, Lin H, Li T, et al. Association between non-alcoholic fatty liver disease and myocardial glucose uptake measured by (18)F-fluorodeoxyglucose positron emission tomography. J Nucl Cardiol. 2020;27:1679–88.
69. Lee HJ, Lee CH, Kim S, Hwang SY, Hong HC, Choi HY, et al. Association between vascular inflammation and non-alcoholic fatty liver disease: Analysis by (18)F-fluorodeoxyglucose positron emission tomography. Metabolism. 2017;67:72–9.
70. Gullberg GT, Shrestha UM, Seo Y. PET imaging of glucose and fatty acid metabolism for NAFLD patients. J Nucl Cardiol. 2020;27:1689–97.
71. Qureshi WT, Alirhayim Z, Khalid F, Al-Mallah MH. Prognostic value of extracardiac incidental findings on attenuation correction cardiac computed tomography. J Nucl Cardiol. 2016;23:1266–74.
72. Goldman LH, Lerer R, Shabrang C, Travin MI, Levsky JM. Clinical significance of incidental findings on coronary CT

angiography: Insights from a randomized controlled trial. J Nucl Cardiol. 2019;27:2306–15.
73. Chiu CZ, Yeh JH, Shyu KG, Hou SM, Lin CL, Liang JA. Can osteoporosis increase the incidence of heart failure in adults? Curr Med Res Opin. 2017;33:1119–25.
74. Fiechter M, Bengs S, Roggo A, Haider A, Marędziak M, Portmann A, et al. Association between vertebral bone mineral density, myocardial perfusion, and long-term cardiovascular outcomes: A sex-specific analysis. J Nucl Cardiol. 2020;27:726–36.
75. Lance Gould K, Bui L, Kitkungvan D, Pan T, Roby AE, Nguyen TT, et al. Pitfalls in quantitative myocardial PET perfusion I: Myocardial partial volume correction. J Nucl Cardiol. 2020;27:386–96.
76. Bui L, Kitkungvan D, Roby AE, Nguyen TT, Gould KL. Pitfalls in quantitative myocardial PET perfusion II: Arterial input function. J Nucl Cardiol. 2020;27:397–409.
77. Poitrasson-Rivière A, Moody JB, Hagio T, Weinberg RL, Corbett JR, Murthy VL, et al. Reducing motion-correction-induced variability in (82)rubidium myocardial blood-flow quantification. J Nucl Cardiol. 2020;27:1104–13.
78. Lassen ML, Rasul S, Beitzke D, Stelzmuller ME, Cal-Gonzalez J, Hacker M, et al. Assessment of attenuation correction for myocardial PET imaging using combined PET/MRI. J Nucl Cardiol. 2019;26:1107–18.
79. Karakatsanis NA, Abgral R, Trivieri MG, Dweck MR, Robson PM, Calcagno C, et al. Hybrid PET- and MR-driven attenuation correction for enhanced (18)F-NaF and (18)F-FDG quantification in cardiovascular PET/MR imaging. J Nucl Cardiol. 2020;27:1126–41.
80. Ather S, Iqbal F, Gulotta J, Aljaroudi W, Heo J, Iskandrian AE, et al. Comparison of three commercially available softwares for measuring left ventricular perfusion and function by gated SPECT myocardial perfusion imaging. J Nucl Cardiol. 2014;21:673–81.
81. Ather S, Iskandrian AE, Hage FG. Sources of variability in the measurement of perfusion defect size using commercially available software programs: Are there gender differences? J Nucl Cardiol. 2017;24:1089–93.
82. Byrne C, Kjaer A, Forman JL, Hasbak P. Reproducibility of LVEF, LV volumes, and LV mass between Rubidium-82 PET/CT scans in young healthy volunteers using two commercially available software packages. J Nucl Cardiol. 2020;27:1237–45.
83. Monroy-Gonzalez AG, Juarez-Orozco LE, Han C, Vedder IR, García DV, Borra R, et al. Software reproducibility of myocardial blood flow and flow reserve quantification in ischemic heart disease: A (13)N-ammonia PET study. J Nucl Cardiol. 2020;27:1225–33.
84. Schindler TH, Valenta I. Relative disagreement among different software packages in PET-flow quantitation: An appeal for consistency. J Nucl Cardiol. 2020;27:1234–6.